Towards in-cell structural study of light-harvesting complexes : an investigation with MAS-NMR

Azadi Chegeni, F.

CHAPTER 4

Conformational dynamics of zeaxanthin-binding LHCII in a lipid membrane

Abstract

Photosynthetic organisms have the challenging task to perform the conversion of light into chemical energy under fluctuating sunlight conditions. To cope with this challenge, they protect themselves from high light by dissipating excess energy as heat via the process called non-photochemical quenching (NPQ). Zeaxanthin (Zea) is essential for the full development of NPQ, but its role remains unclear. This chapter addresses the molecular effects of Zea on the structure and dynamics of Light Harvesting Complex II (LHCII). We applied solid state NMR spectroscopy on LHCII from the *npq2* mutant, which binds Zea in the V1 binding pocket, to investigate the effect of Zea on the protein conformational dynamics. Our results demonstrate that *npq2* LHCII have a different conformation than wildtype LHCII, from which we conclude that the protein fold and pigment-protein dynamics of LHCII depends on its oligomerization state and/or xanthophyll (Zea) binding. Moreover, we observe that, in contrast to wildtype LHCII, *npq2* LHCII contains a significant number of intrinsic galactolipids that are strongly bound. We conclude that Zea binding and monomerization influence lipid binding to LHCII and thereby could also influence structural arrangements and dynamics on the membrane level.

Introduction

In excess light, the process of non-photochemical quenching (NPQ) is activated that causes heat dissipation of chlorophyll (Chl) excited-state energies in the Photosystem II (PSII) antenna. Two important components of NPQ are the pH-activated quenching of excitations in the light-harvesting antenna, known as qE, and zeaxanthin (Zea) dependent quenching, known as qZ, that is activated by the xanthophyll cycle which reversibly converts the carotenoid violaxanthin (Vio) into Zea via antheraxanthin. Molecular sites involved in qE and qZ are integrated in the Chl *a*/*b* binding light-harvesting antenna complexes of PSII, of which the most abundant ones are the LHCII. LHCII pigment-protein complexes are membrane proteins that bind various Chl *a* and *b* and different types of carotenoids in conserved binding pockets for lutein (L1 and L2), neoxanthin (N1) and violaxanthin (V1). In the xanthophyll cycle process, Vio in the V1 binding site of LHCII are replaced by Zea. Figure 1 presents the monomeric crystal structure of LHCII, highlighting the carotenoid binding sites.

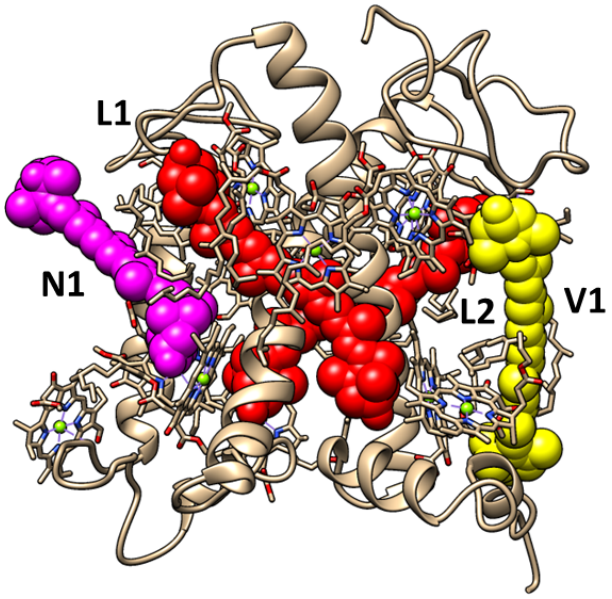

Figure 1. Crystal structure of monomeric LHCII indicating the carotenoid binding pockets. Neoxanthin (N1) is highlighted in purple, luteins (L1 and L2) are highlighted in red and violaxanthin (V1) in yellow.

The molecular effect of Zea replacement in LHCII is unclear. Zea might act directly with Chls in the antenna and quench excitations by Chl to Zea energy transfer or by forming charge-transfer states [1]. In its role as allosteric regulator of qE, Zea binding might promote a conformational change in LHCII due to its more hydrophobic nature [2-3]. Alternatively it has been proposed that Zea could be acting in between the complexes in the thylakoid membrane, to create a variety of quenching sites in the antenna complexes [4]. The presence of Zea appears to have a rigidifying effect on membrane fluidity and several experiments suggest that Zea binding rigidifies LHCII and stabilizes its quenched state [5]. However, structural data underpinning these structural effects are lacking.

The *npq2* mutants bind consitutely Zea in the V1 binding pocket of LHCII and provide an effective way to study the effect of Zea on structure and dynamics of LHCII. The *npq2* mutants lack the antheraxanthin enzyme to convert the Zea back to Vio in the V1 pocket, and also lack the carotenoid neoxanthin.

We performed a 2D dipolar based and INEPT based NMR analysis of Zea-containing LHCII complexes that were reconstituted in liposome membranes. ^{13}C-^{15}N isotope-labeled LHCII complexes were isolated from the *npq2* strain of *Chlamydomonas reinhardtii* (*Cr.*). The liposomes for protein insertion were

composed of MGDG, DGDG, SQDG and PG. The lipid composition was chosen to mimic the lipid composition of native thylakoid membranes and a protein to lipid ratio of 1:55 (mol:mol) was chosen to mimic native protein packing densities [6]. These conditions are identical to those that we used in a study of WT LHCII proteoliposomes by NMR spectroscopy (Chapter 3). The collected ^{13}C-^{13}C PARIS and ^{13}C-^{13}C INEPT-TOBSY solid-state NMR spectra of Zea-LHCII proteoliposomes were compared to the previously collected spectra of wild type (WT) LHCII and show remarkable differences in structure, internal protein dynamics and lipid binding.

Material and Methods

LHCII extraction

Cr. Strains of *npq2* were grown under conditions as previously described for the WT cells in chapter 2. After thylakoid isolation, *Cr. npq2* thylakoids were re-suspended in buffer (50 mM Hepes-KOH pH 7.5, 5 mM $MgCl_2$ with 50% glycerol). For isolation of the LHCII fractions, thylakoid membranes corresponding to 3 mg/ml of total chlorophylls (based on the optical density at 680 nm) were washed with 50 mM EDTA and solubilized for 20 minutes on ice in 3 ml of 1.2% α-DM in 10 mM Hepes (pH 7.5), after vortexing for 1 minute. The solubilized samples were centrifuged at 15000×g for 30 minutes to eliminate any unsolubilized material and the supernatant with the photosynthetic complexes was then fractionated by ultracentrifugation in a 0–1 M sucrose gradient containing 0.06% α-DM and 10 mM Hepes (pH 7.5), at 141000×g for 40 hours at 4 ℃. The green fraction corresponding monomeric *npq2* LHCII proteins was harvested with a syringe and the Chl concentration was adjusted to 2 mg/ml with buffer (50 mM HEPES, 5 mM $MgCl_2$, pH 7.5).

Preparation of liposomes

Npq2 LHCII proteins solubilized in α-DM were reconstituted in lipid membranes of which the lipid composition mimics the native thylakoid membrane. The proteoliposomes contained 47% MGDG, 12% SQDG, 14% PG and 27% DGDG at a protein-to-lipid ratio of 1:55 [7]. The chosen protein to lipid ratio is in the range of native protein packing densities in thylakoid membranes, where 70-80% of the membrane surface area is occupied by proteins [6]. The lipids were dissolved in chloroform and dried into a thin film using a rotary evaporator at 40 °C. The lipid film was hydrated by reconstitution buffer (50mM HEPES,

5mM Mgcl2, pH=7.5 and 0.03% β-DM) and were exposed to 10 freeze-thaw cycles. After that, *npq2* LHCII was inserted into liposomes and detergent was removed by 72 hours of dialysis against detergent-free buffer. During the dialysis bio beads (SM-2, Bio Rad) were added to the buffer to speed up the dialysis process.

Pigment analysis

The content of individual carotenoids of *npq2* LHCII was determined using high performance liquid chromatography (HPLC, Beckman System Gold), as described in [8]. The peaks of each sample were identified through the retention time and absorption spectrum [9].

UV/Visible spectroscopy

Absorption spectra were recorded on a Cary 60 UV–visible spectrophotometer (Agilent Technologies) with the wavelength range set from 350 to 750 nm using 0.5 cm cuvettes.

Time-resolved fluorescence spectroscopy (TRF)

TRF measurements were performed using a FluoTime 300 (PicoQuant) time-correlated photon counter spectrometer. Samples were hold in a 1x1 cm quartz cuvette that was kept at 20 ^{o}C with a thermostat and excited at 440 nm using a diode laser (PicoQuant). Fluorescence decay traces were fitted with multi-exponentials using a χ^2 least-square fitting procedure.

NMR sample preparation

For the NMR samples, 18 ml of *npq2* LHCII proteoliposomes, containing approximately 6 mg LHCII and 1.5 mg Chl (as determined by OD_{680} of the Chls), was pelleted by ultra-centrifugation (223000×g, 4 ^{o}C, 90 min) and transferred to a thin-wall 3.2 mm solid-state NMR MAS (Magic Angle Spinning) rotor through centrifugation.

Solid-State NMR experiments

Solid-state NMR spectra were recorded with an ultra-high field 950-MHz ^{1}H Larmor frequency spectrometer (Bruker, Biospin, Billerica) equipped with a triple-channel ^{1}H, ^{13}C, ^{15}N 3.2 mm MAS probe. ^{13}C -^{13}C PARIS and ^{13}C-^{13}C INEPT on ^{13}C-^{15}N *npq2* LHCII in lipid bilayers were recorded under the same MAS frequency, temperature and parameters as ^{13}C-^{15}N WT LHCII in lipid bilayers (chapter 3). Typical $\pi/2$ pulses were 3 μs for ^{1}H, 5 μs for ^{13}C, and 8 μs for

^{15}N. The ^{1}H/^{15}N and ^{1}H/^{13}C cross-polarization (CP)[10] contact times were 800 µs and 1 ms, respectively, with a constant radio frequency (rf) field of 35 and 50 kHz on nitrogen and carbon, respectively, while the proton lock field was ramped linearly around the *n*=1 Hartmann/Hahn condition[11]. The ^{15}N/^{13}Ca SPECIFIC-CP transfer[12] was implemented with an optimized contact time of 4.2 ms with a constant lock field of 2.5×ν_r applied on ^{15}N, while the ^{13}C field was ramped linearly (10% ramp) around 1.5×ν_r. ^{1}H decoupling during direct and indirect acquisition was performed using SPINAL64 [13] with ~83 kHz irradiation. The presented 2D ^{13}C-^{13}C PARIS[14] spectra were collected with a mixing time of 30 ms at 17 kHz MAS at a set temperature of -18 °C. The *J*-coupling based 2D ^{13}C-^{13}C INEPT-TOBSY[15-16] experiments were recorded at -3 °C with TOBSY mixing of 6 ms at 14 kHz MAS. Spectra were processed with Bruker TopSpin 3.2 (Bruker, Germany) with LPfr linear prediction and fqc mode for Fourier transformation. Spectra were analyzed by Sparky version 3.114[17] and MestReNova 11.0 (Mestrelab Research SL, Santiago de Compostela, Spain).

Results

Biochemical analysis of *npq2* LHCII sucrose gradient analysis shows that the NPQ2 LHCII has a reduced trimeric content with respect to the WT (CW15) strain, as reported in literature [18-21], and consequently monomeric fractions were collected. The inability to synthesize antheraxanthin, violaxanthin and neoxanthin and the constitutive accumulation of Zea in the Vx binding pocked was confirmed by high-pressure liquid chromatography (HPLC) analysis (see figure 2). The sucrose gradient analysis in figure 2A is also shown in chapter 2, figure 1, but is presented here again for discussion on the molecular properties of *npq2* LHCII. For comparison with the wild type LHCII, the *npq2* HPLC data is shown together with the HPLC chromatogram of wild type LHCII that was already presented in chapter 3, figure 3.

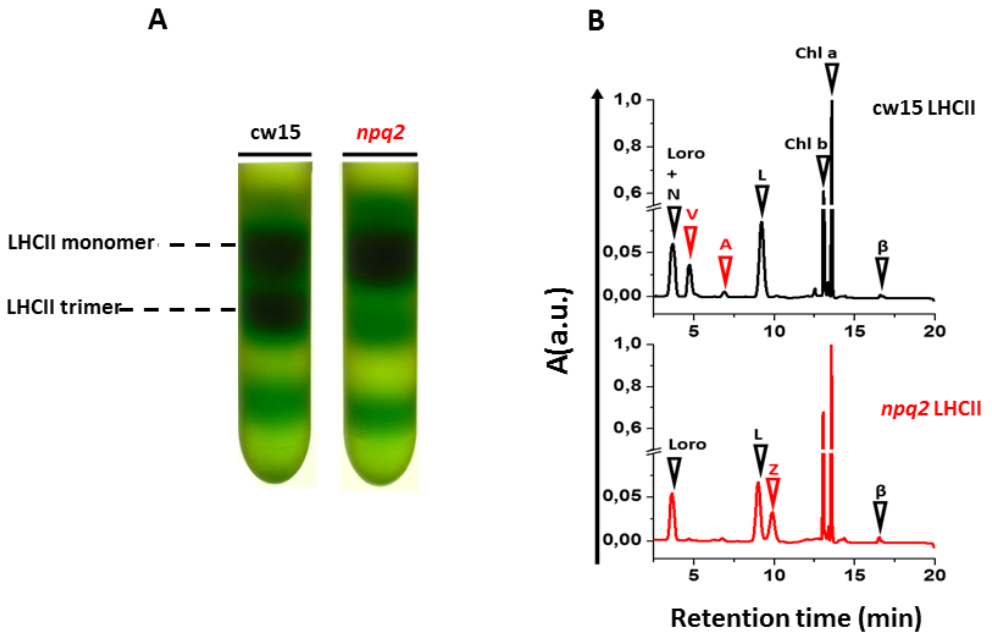

Figure 2. A: LHCII purification from sucrose gradients of thylakoid membranes from WT (CW15) and *npq2 Cr.* cells. **B:** HPLC analysis of WT trimeric LHCII and *npq2* monomer LHCII fractions. Data of figure 2A has also been presented in Chapter 2, figure 1 and the HPLC chromatogram of the WT LHCII has also been presented in Chapter 3, figure 3.

In order to mimic the native lipid environment and to be consistent with conditions that were used for NMR analysis of WT LHCII, *npq2* LHCII was inserted into liposomes prepared from MGDG, DGDG, SQDG and PG lipids with a protein to lipid ratio of 1:55. Under these conditions, the LHCII complexes form aggregates inside the membranes and consequently the proteoliposomes are strongly fluorescence quenched, as shown in the time-resolved data in figure 3A. The *npq2* LHCII in α-DM has an average life time of 3.2 ns, confirming that Zea binding to LHCII in itself does not induce a quenched state. The average lifetime is reduced to 1.1 ns after insertion into liposomes. The fluorescence characteristics are similar to those of the WT LHCII proteoliposomes that are reported in chapter 3 and that reveal similar strong fluorescence quenching which is attributed to aggregation of LHCII in the membranes. In addition, absorption spectra of the *npq2* LHCII were collected before and after insertion into the liposomes and are shown in figure 3B.

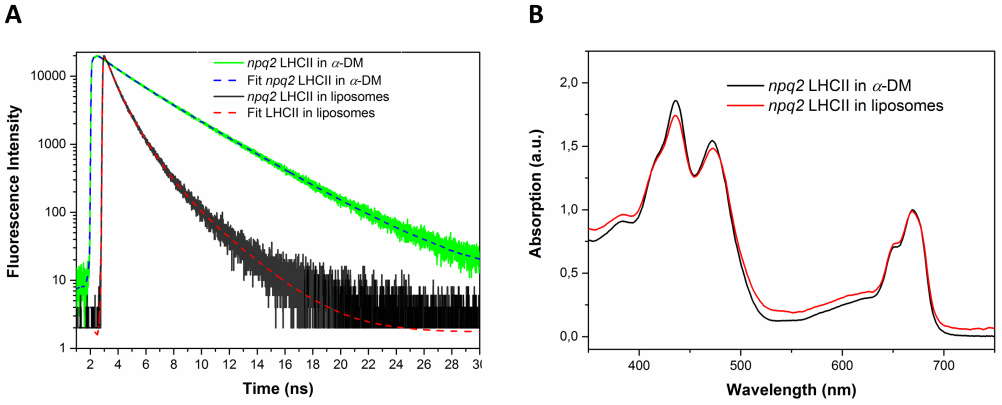

Figure 3. A: Time resolved fluorescence of *npq2* LHCII in α-DM detergent (green) and *npq2* LHCII in liposomes (black). **B:** Absorption spectra of *npq2* LHCII in α-DM detergent (black) and after inserting into liposomes (red).

Dipolar-based ssNMR experiments

Solid state NMR techniques were employed for investigation of the effect of Zea on the structure and dynamics of LHCII in lipid bilayers. First, 2D ^{13}C-^{13}C dipolar based PARIS spectra were collected on the ^{13}C-^{15}N *npq2* LHCII proteoliposomes under conditions described in the Materials and Methods section and results were compared to the spectra of ^{13}C-^{15}N WT LHCII proteoliposomes that were collected at identical experimental conditions.

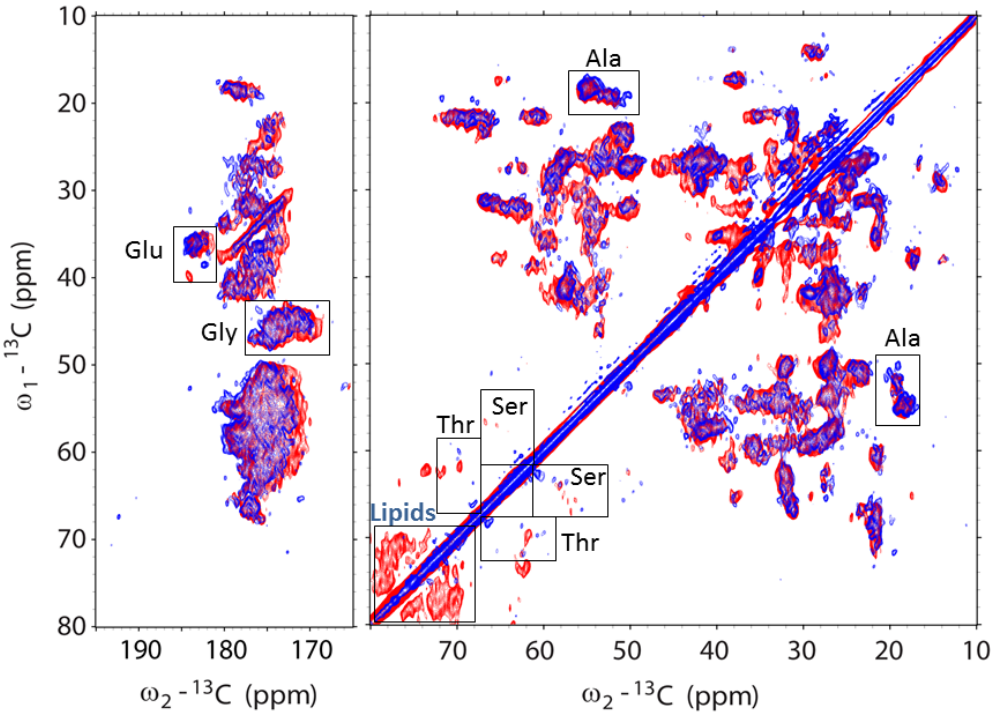

Figure 4. Overlaid ^{13}C -^{13}C PARIS spectra of WT LHCII (blue) and *npq2* LHCII (red). Spectra were collected at 255K and with 17 kHz MAS spinning.

Figure 4 shows the dipolar-based ^{13}C-^{13}C spectra of WT LHCII (blue) overlaid with *npq2* LHCII (red) that were collected and processed under identical conditions. The strong overlap of two spectra confirms that the overall fold of LHCII is preserved when Vio is replaced by Zea. However, the resonance peaks in the spectrum of *npq2* LHCII seem severely broadened. A readout temperature of 255K was applied for comparison with the WT LHCII spectrum under matching conditions. The CC PARIS experiments on *npq2* LHCII were repeated at 270K, which significantly improved the spectral resolution in the lipid region (figure 5 and 6).

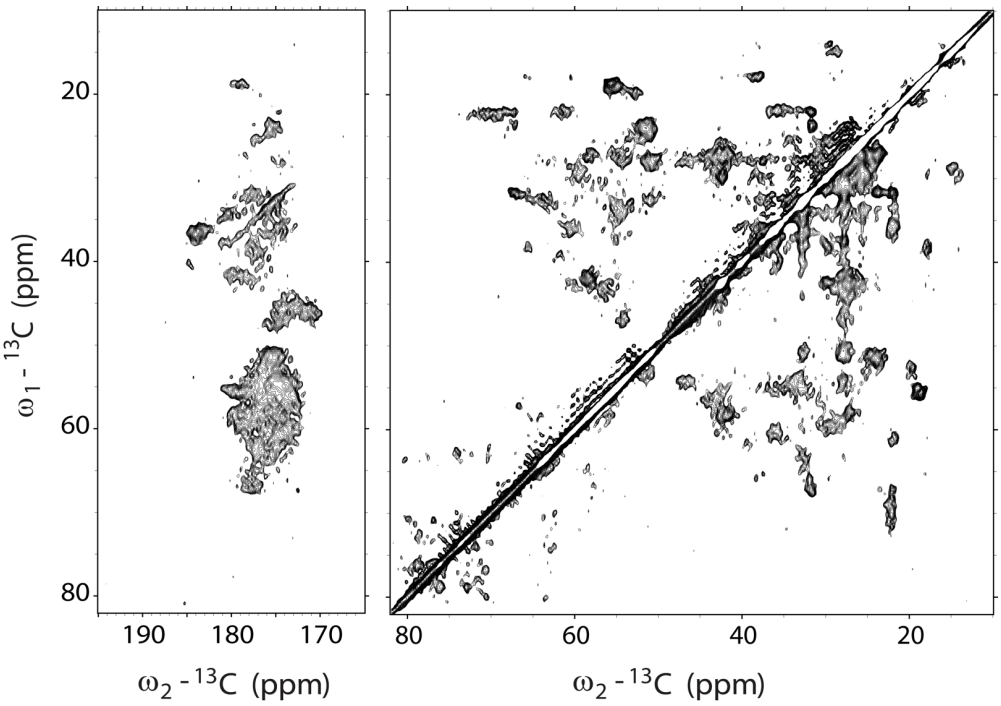

Figure 5. ^{13}C-^{13}C PARIS spectra of *npq2* LHCII at 270 K and 17 kHz MAS spinning.

Another clear difference between the *npq2* and the WT LHCII spectrum as shown in the figure 4 and 6A, is the presence of strong signals resonating between 70-80 and 105 ppm in the spectrum of *npq2* LHCII that are from signals from the galactolipid heads. Since the liposome lipids are not isotope-labeled and the probability for detecting ^{13}C-^{13}C correlations among natural abundance ^{13}C carbons is very low, lipid signals must arise from intrinsic thylakoid lipids that remained associated with LHCII upon its purification. According to galactolipid head chemical-shift assignments, signals around 105-107 ppm originate from the galactosyl C1' carbon of MGDG or DGDG, correlating with C2', C3' or C4' around 73-77 ppm. DGDG molecules should give additional signals from the second ring with chemical shifts of C1" around 101 ppm. Because no additional correlations are observed, we tentatively attribute the strong lipid galactosyl signals to MGDG molecules that are strongly bound to Zea-LHCII and must be non-annular lipids that do not exchange on NMR time scales (*i.e.* $< 10^4\ s^{-1}$).

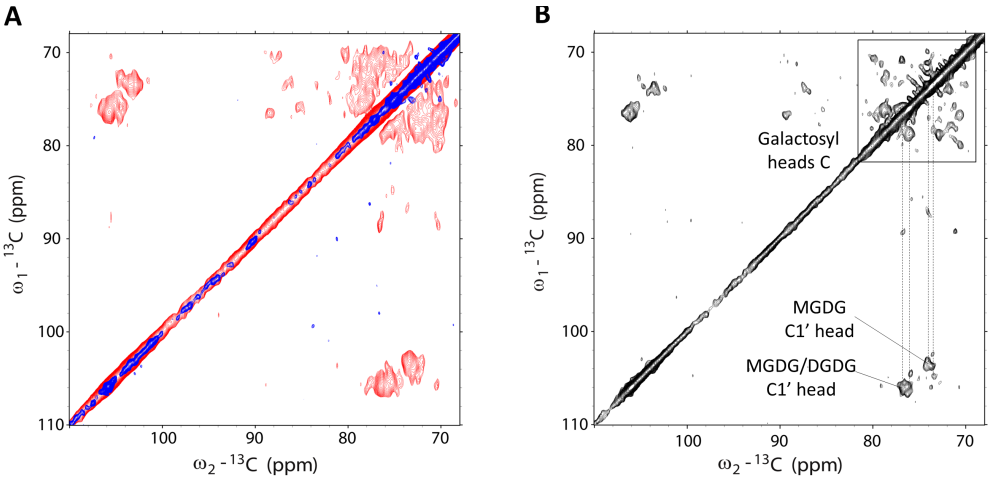

Figure 6. A: Close up of lipid signals in ^{13}C -^{13}C PARIS spectrum of WT (blue) and *npq2* (red) LHCII at 255K. **B:** ^{13}C -^{13}C PARIS spectrum of *npq2* LHCII at 270K.

For further analysis of the *npq2* LHCII backbone structure, we take a closer inspection of selective spectral regions. The backbone C_α and C_β chemical-shift signals of Ala, Thr and Ser residues accumulate in distinct spectral regions that are separated from the correlations of other amino acid residues. Comparing the Ala, Ser and Thr backbone chemical shifts of *npq2* LHCII to the shifts of the WT LHCII, significant differences are observed. Three clear Ala C_α-C_β correlations in the WT LHCII spectrum are lacking in the *npq2* LHCII spectrum as indicated in figure 7B. These three peaks in the spectrum of WT LHCII do not match with any predicted chemical-shift correlations that were produced using *Cr* LHCII structure homology models (chapter 3). The homology models are built from the plant LHCII X-ray structures that lack the first 14 residues in the N terminus and therefore the three peaks could be from Ala residues in the N-terminal stretch. Also in the Thr and Ser coil regions of C_α-C_β correlations, dramatic changes are observed (figure 7B). While the Thr and Ser coil signals in the WT spectrum are rather weak, multiple strong signals are observed in the *npq2* spectrum. In addition, interesting changes in the chemical shift pattern of Ser residues are observed (figure 7A). According to the crystal structure, LHCII consists of three transmembrane helixes together with large flexible loops and tails. However, several Ser residues of *npq2* LHCII appear to have strand conformations according to the PARIS NMR spectrum. This suggests that *npq2* LHCII folds into strands in some parts of the protein. Thr and Ser residues in the coil area are highlighted in red in the crystal structure of LHCII (figure 8).

Furthermore, in the CO region of the spectrum, we observe a clear change in the NMR signal of a Glu COO^- carboxyl side chain that indicates a change in one of the Glu residues in the *npq2* LHCII (figure 7C).

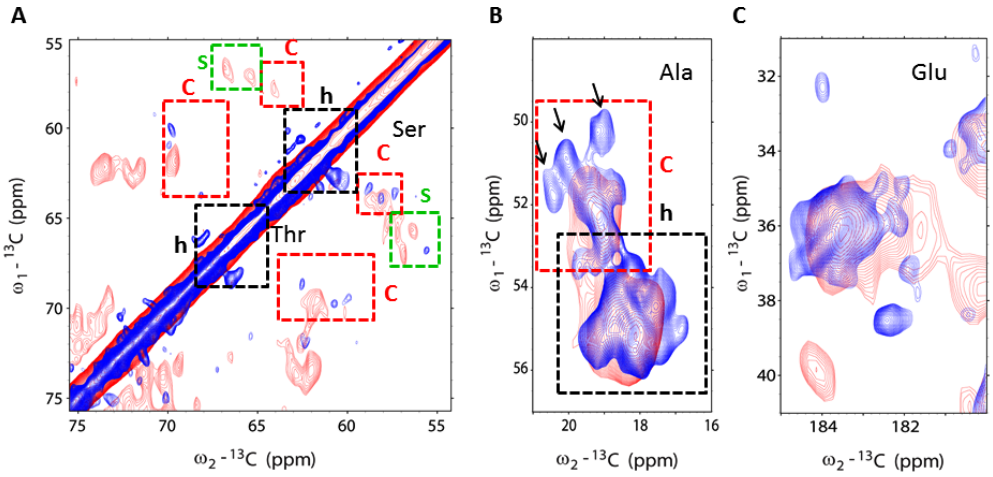

Figure 7. **A:** The Ser and Thr regions in the ^{13}C -^{13}C PARIS spectra of WT (blue) and *npq2* (red) LHCII. Helix, coil and β strands contribution are presented with black, red and green boxes. **B:** The Ala region. Arrows indicate extra resonances that are observed in the spectrum of WT LHCII. **C:** Glu COO region.

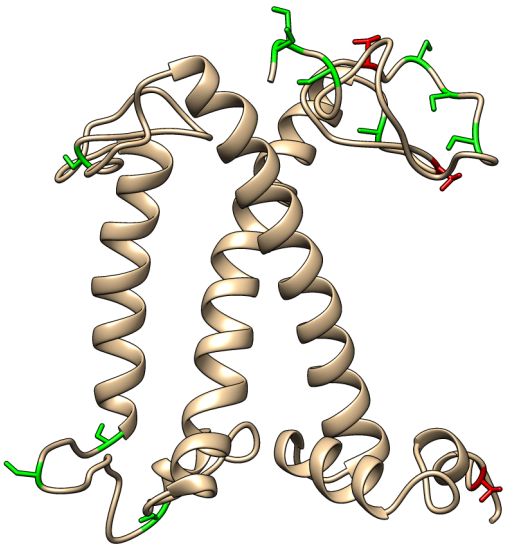

Figure 8. Crystal structure of LHCII highlighting the Thr (red) and Ser (green) residues in coil regions.

Several carotenoid and Chl pigment correlations can easily be identified in the spectra because they accumulate in a spectral region where no protein signals occur, including the carotenoid conjugated-chain CH_3-CH correlations and correlations of the Chl *a* $C8^1/8^2$– 8/9 macrocycle side chains (figure 9). By comparison with NMR data of U-^{13}C-lutein LHCII (Crisafi *et al.*, in progress), we are able to attribute the most upfield shifted carotenoid CH chemical shifts below 132 ppm to Zea. In the *npq2* mutant, the only carotenoids that are present are lutein and Zea. In WT spectra the chemical shift changes are observed for Chl *a* $C8^1/8^2$– 8/9 resonances, however in *npq2* spectra the signals appear shifted to upfield. According to the crystal structure of LHCII, Chl *a* 614 is close proximity to the Zea molecule and close interaction between Zea and Chl *a* 614 might explain the different Chl *a* shift pattern compared to the spectrum of WT LHCII.

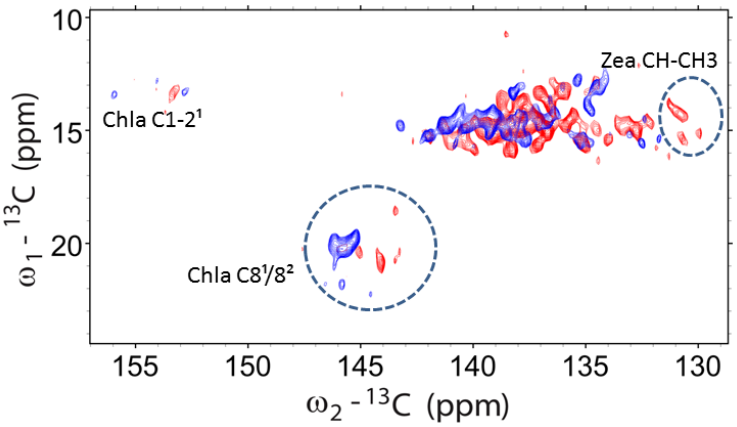

Figure 9. Pigment region of the ^{13}C-^{13}C PARIS spectrum of WT (blue) and *npq2* (red) LHCII. Circles indicate the upfield shifted of carotenoid and Chl *a* signals.

J-coupling based ssNMR experiments

The conformational dynamics of *npq2* LHCII is further investigated by a 2D ^{13}C-^{13}C INEPT-TOBSY experiment that was collected at 270K. In this experiment polarization transfer is based on *J*-coupling interactions and that is selective for molecules that undergo strong ns or sub-ns motions. Selective protein signals are observed in the *npq2* INEPT spectrum that overlap with the INEPT-TOBSY spectrum of the WT (figure 10). However, for a Phe and two Thr residues, and two Chl phytol chains, signals are observed in the WT INEPT spectrum but not in the INEPT spectrum of *npq2* LHCII. The Chl tails were predicted to belong to

Chl605 and Chl606 that of which the tails are not resolved in the X-ray structures and the Phe residue was predicted to be located in the LHCII C terminus (chapter 3). In addition, few other protein signals are few shifted or missing in the *npq2* spectrum compared to the WT spectrum as indicated by circles in figure 10. Furthermore, the *npq2* spectrum shows resonances of lipid galactosyl heads that are also observed in the WT spectrum. These signals are attributed to lipids that have been co-purified with LHCII, but are not strongly bound and may have exchanged with bulk lipids upon reconstitution of LHCII in the liposomes.

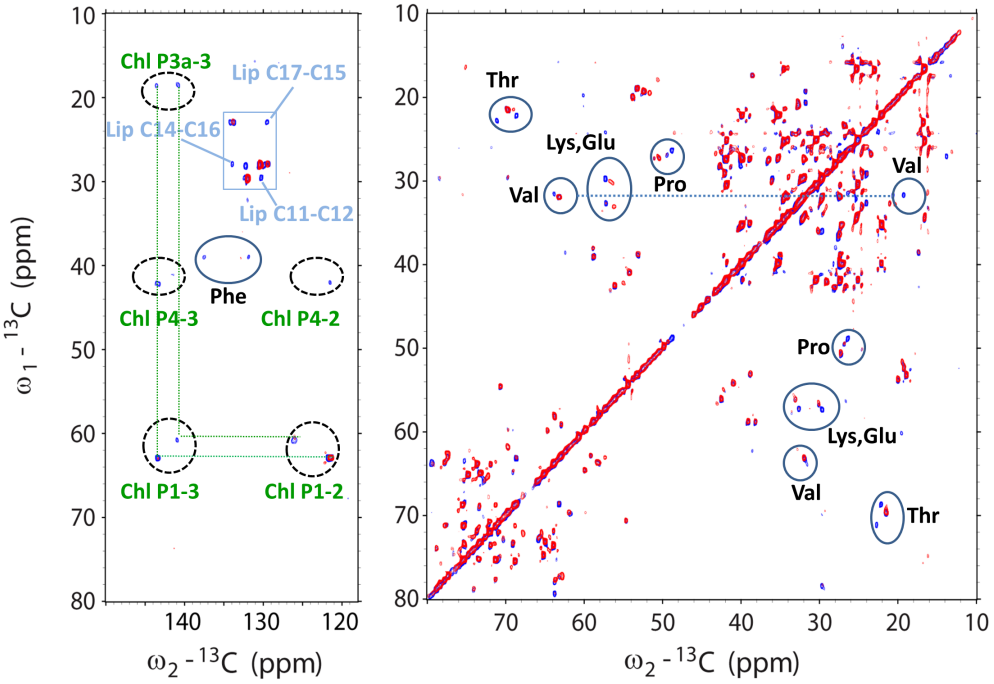

Figure 10. Overlaid ^{13}C-^{13}C INEPT-TOBSY spectra of WT (blue) and *npq2* (red) LHCII. Spectra were collected with a spinning frequency of 14 kHz at 270K. Resonance signals of residues which are missing or shifted in the *npq2* spectra are indicated with circles.

Discussion

The analyzed *npq2* LHCII complex differs in three ways from the WT complex: (i) Vio is replaced by Zea, (ii) the Neo carotenoid that points outwards the complex is lacking, and (iii) due to destabilization of the trimers in *npq2*

membranes, the *npq2* LHCII complexes were collected as monomers. The strong signals in the CP-based NMR spectrum of non-annular galactolipids associated with *npq2* LHCII contrast with the picture of lipids associated with WT LHCII. For the WT complexes only a small number of associated galactolipids were detected, and only in INEPT-based spectra, indicating that those lipids were not tightly bound and likely are annular lipids (chapter 3) [22]. The difference may be explained by the monomerization of *npq2* LHCII. Compared to trimers, LHCII monomers will have more membrane-exposed hydrophobic protein sites that form potential lipid binding sites. Another possible explanation is that Zea increases the affinity of LHCII for lipids, owing to its more hydrophobic nature compared to Vio. It is not clear if the LHCIIs are already present as monomers in the *npq2* thylakoid membranes or that lower stability of *npq2* LHCII trimers caused their monomerization during purification. For WT LHCII, light-induced trimer to monomer transitions have been observed [23] and it is has been reported that high light induces monomerization of LHCII trimers in plant leaves, leading to more quenching and less efficient transfer of excitations to the reaction center [24]. The monomeric state of LHCII, or oligomers formed from LHCII monomers, thus represents a state that may also be present under stress conditions *in vivo*. The recently obtained cryo-EM LHCII-PSII supercomplex structures reveal well-defined lipid molecules that contribute to interactions between the LHCII and PSII core [25]. Increased lipid binding to monomeric Zea LHCII could play a role in modulating LHCII-PSII interactions, or the interactions among the antenna proteins. Moreover, it has been reported that elevated levels of Zea associated with LHCII oligomers enhances resistance to photooxidative stress by a lipid-protective mechanism [26]. Increased affinity of lipids for Zea-containing LHCII could also serve as a way to protect thylakoid lipids under light stress conditions.

It is very interesting to note that also 2D CP-PARIS NMR spectra of *Cr. npq2* whole thylakoids from which the *npq2* LHCII were isolated differ from WT thylakoid spectra by containing strong signals of immobilized galacolipid heads (chapter2) [22]. This suggests that also inside the original *npq2* thylakoid membranes galactolipids are strongly associated with Zea LHCII. We speculate that those lipids bound to Zea LHCII count for the additional fraction of immobilized lipids that is observed in *npq2* thylakoids compared to WT thylakoids[22] and may contribute to the overall rigidity of Zea-containing thylakoid membranes as has been described in chapter 2 and by various other reports [18, 27].

In INEPT spectra of WT LHCII proteoliposomes, Chl phytol tail signals are detected that were attributed to Chl *b* 605 and 606. The 605 and 606 Chls are located at the periphery of the complexes and have Chl tails that will protrude

into the surrounding lipid bilayer. Dynamic Chl tails are only detected for WT and not for *npq2* LHCII, indicating that WT LHCII has a less tight packing in the proteoliposome membranes. Other dynamic sites that are detected for WT but not for *npq2* LHCII involve two Thr and one Phe residue. In our previous study, we predicted that these dynamic amino acids are located in the C terminus, which site is involved in stabilizing the V1 carotenoid. The reduced dynamics of this site in *npq2* LHCII suggests that Zea in the V1 pocket rigidifies the LHCII protein structure. This notion is further confirmed by strong Thr and Ser coil and strand signals that appear in the *npq2* spectrum, while the Thr and Ser coil signals in the CP-PARIS spectrum of WT LHCII are very weak.

The three coil Ala peaks in the LHCII WT spectrum that are not found in the *npq2* spectrum could originate from the N terminal stretch, which would suggest that the N terminal stretch adopts a more ordered structure in WT LHCII. Furthermore, the LHCII crystal structures do not contain strand segments, while the NMR spectrum of *npq2* LHCII contains Ser signals in the predicted region for strand conformations. These differences clearly indicate that the LHCII pigment-protein complex has sites with structural plasticity that refold upon xanthophyll exchange and/or monomerization.

Conclusion

In summary, our results provide converging evidence for structural plasticity in LHCII. The same protein matrix adopts a different fold depending on its trimerization state, and on Zea binding in the V1 pocket. Both elements also have a strong effect on the lipid affinity of LHCII and may affect the overall membrane fluidity or supramolecular organization by changes in lipid-protein interactions.

References

1. Holt, N. E.; Zigmantas, D.; Valkunas, L.; Li, X.; Niyogi, K.; Fleming, G. R., Carotenoid Cation Formation and the Regulation of Photosynthetic Light Harvesting. *Science* **2005,** *307*, 433-436.
2. Ruban, A.; Ruban, M.; Duffy, The photoprotective molecular switch in the photosystem II antenna. *Biochimica et biophysica acta. Bioenergetics* **2012,** *1817* (1), 167-181.

3. Horton, P.; Ruban, A. V.; Wentworth, M., Allosteric regulation of the light-harvesting system of photosystem II. *Philos Trans R Soc Lond B Biol Sci* **2000,** *355* (1402), 1361-70.
4. Xu, P.; Tian, L.; Kloz, M.; Croce, R., Molecular insights into Zeaxanthin-dependent quenching in higher plants. *Scientific Reports* **2015,** *5*, 13679.
5. Schlau-Cohen, G. S.; Yang, H. Y.; Kruger, T. P.; Xu, P.; Gwizdala, M.; van Grondelle, R.; Croce, R.; Moerner, W. E., Single-Molecule Identification of Quenched and Unquenched States of LHCII. *J Phys Chem Lett* **2015,** *6* (5), 860-7.
6. Kirchhoff, H.; Mukherjee, U.; Galla, H. J., Molecular architecture of the thylakoid membrane: lipid diffusion space for plastoquinone. *Biochemistry* **2002,** *41* (15), 4872-82.
7. Crisafi, E.; Pandit, A., Disentangling protein and lipid interactions that control a molecular switch in photosynthetic light harvesting. *Biochim Biophys Acta* **2017,** *1859* (1), 40-47.
8. Färber, A.; Jahns, P., The xanthophyll cycle of higher plants: influence of antenna size and membrane organization. *Biochim. Biophys. Acta* **1998,** *1363*, 47-58.
9. Jeffrey, S. W.; Mantoura, R. F. C.; Wright, S. W., Phytoplankton pigments in oceanography: guidelines to modern methods. *Monogr. Oceanogr. Methodol.* **1997**.
10. Pinest, A.; Gibbyt, M.G.; Waugh, J. S., Proton-enhanced NMR of dilute spins in solids. *The journal of Chemical Physics* **1973,** *69* (2), 569-590.
11. Hartmann, S. R.; Hahn, E. L., Nuclear Double Resonance in the Rotating Frame. *Physical Review* **1962,** *128* (5), 2042-2053.
12. Baldus, M.; Petkova, A. T.; Herzfeld, J.; Griffin, R. G., Cross polarization in the tilted frame: assignment and spectral simplification in heteronuclear spin systems. *Molecular Physics* **1998,** *95* (6), 1197-1207.
13. Fung, B. M.; Khitrin, A. K.; Ermolaev, K. An Improved Broadband Decoupling Sequence for Liquid Crystals and Solids. *Journal of Magnetic Resonance* **2000,** *142*, 97-101.
14. Weingarth, M.; Demco, D. E.; Bodenhausen, G.; Tekely, P., Improved magnetization transfer in solid-state NMR with fast magic angle spinning. *Chemical Physics Letters* **2009,** *469* (4-6), 342-348.
15. Baldus, M.; Meier, B. H., Total Correlation Spectroscopy in the Solid State. The Use of Scalar Couplings to Determine the Through-Bond Connectivity. *Journal of Magnetic Resonance, Series A* **1996,** *121* (1), 65-69.
16. Morris, G. A.; Freeman, R., Enhancement of nuclear magnetic resonance signals by polarization transfer. *J. Am. Chem. Soc* **1979,** *101* (3), 760–762.
17. Goddard, T.; Kneller, D., SPARKY. *University of California, San Francisco*.
18. Tardy, F.; Havaux, M., Thylakoid membrane fluidity and thermostability during the operation of the xanthophyll cycle in higher-plant chloroplasts. *Biochimica et biophysica acta* **1997,** *1330* (2), 179-93.
19. Lokstein, H.; Tian. L ;Polle, J. E. W.; DellaPenna, D., Xanthophyll biosynthetic mutants of Arabidopsis thaliana: altered nonphotochemical quenching of chlorophyll £uorescence is due to changes in Photosystem II antenna size and stability. *Biochimica et Biophysica Acta* **2002,** *1553*, 309-319.
20. Havaux, M.; Dall'Osto, L.; Cuine, S.; Giuliano, G.; Bassi, R., The effect of zeaxanthin as the only xanthophyll on the structure and function of the photosynthetic apparatus in Arabidopsis thaliana. *J Biol Chem* **2004,** *279* (14), 13878-88.
21. Dall'Osto, L.; Caffarri, S.; Bassi, R., A mechanism of nonphotochemical energy dissipation, independent from PsbS, revealed by a conformational change in the antenna protein CP26. *Plant Cell* **2005,** *17* (4), 1217-32.
22. Azadi Chegeni, F.; Perin, G.; Sai Sankar Gupta, K. B.; Simionato, D.; Morosinotto, T.; Pandit, A., Protein and lipid dynamics in photosynthetic thylakoid membranes investigated by in-situ solid-state NMR. *Biochim Biophys Acta* **2016,** *1857* (12), 1849-1859.

23. Garab. G1; Cseh. Z; Kovács. L; Rajagopal. S; Várkonyi. Z; Wentworth. M; Mustárdy. L; Dér. A; Ruban. A.V; Papp. E; Holzenburg. A; P., H., Light-Induced Trimer to Monomer Transition in the Main Light-Harvesting Antenna Complex of Plants: Thermo-Optic Mechanism. *Biochemistry* **2002,** *41*, 15121-15129.
24. Bielczynski, L. W.; Schansker, G.; Croce, R., Effect of Light Acclimation on the Organization of Photosystem II Super- and Sub-Complexes in Arabidopsis thaliana. *Front Plant Sci* **2016,** *7*, 105.
25. Lu, S.; Cao, Y.; Fan, S. B.; Chen, Z. L.; Fang, R. Q.; He, S. M.; Dong, M. Q., Mapping disulfide bonds from sub-micrograms of purified proteins or micrograms of complex protein mixtures. *Biophys Rep* **2018,** *4* (2), 68-81.
26. Johnson, M. P.; Havaux, M.; Triantaphylides, C.; Ksas, B.; Pascal, A. A.; Robert, B.; Davison, P. A.; Ruban, A. V.; Horton, P., Elevated zeaxanthin bound to oligomeric LHCII enhances the resistance of Arabidopsis to photooxidative stress by a lipid-protective, antioxidant mechanism. *J Biol Chem* **2007,** *282* (31), 22605-18.
27. Havaux, M., Carotenoids as membrane stabilizers in chloroplasts. *trends in plant science* **1998,** *3*, 147-151.